A Protection and Detection Surface (PADS) for Damage Tolerance

Mark J. Shuart
*Langley Research Center
Hampton, Virginia*

Chunchu B. Prasad
*Analytical Services & Materials, Inc.
Hampton, Virginia*

Sherrill B. Biggers
*Lockheed Aeronautical Systems Company
Burbank, California*

The use of trademarks or names of manufacturers in this report is for accurate reporting and does not constitute an official endorsement, either expressed or implied, of such products or manufacturers by the National Aeronautics and Space Administration.

Summary

A concept for a protection and detection surface (PADS) has been studied for application to composite primary aircraft structures. A Kevlar-epoxy woven face sheet with a Rohacell foam core was found to be the most effective PADS configuration among the configurations evaluated. The weight of the PADS configuration was estimated to be approximately 17 percent of the structural weight. The PADS configuration was bonded to graphite-epoxy base laminates, and up to a 70-percent improvement was observed in compression-after-impact failure strains.

Introduction

Cost-effective, weight-efficient composite structures should also be damage tolerant. Damage tolerance for composite structures has been achieved using a materials approach (e.g., tough material systems (refs. 1–3)) and/or a structures approach (e.g., structural concepts having redundant load paths (ref. 4)). These approaches minimize the structural performance degradation due to damage by minimizing the extent of damage propagation. However, these approaches do not contribute to damage detectability during routine inspection. The indetectability of damage can dominate the design criteria for some structural components. A simple approach is needed that both minimizes performance degradation and indicates the location of potential damage.

The current investigation was conducted to study a concept for a protection and detection surface (PADS) for application to composite primary aircraft structures. This PADS concept utilizes a lightweight sandwich construction that can be applied to the outer surface of a structure. The PADS concept protects a structure from critical impact events by absorbing impact energy and enables simple and reliable detection of the location of potential point-source damage. A preliminary study was conducted to identify effective PADS constituents and to evaluate the behavior of composite laminates with the PADS concept. The performance of the PADS constituents was evaluated on the basis of damage visibility and damage protection. The best performing design was selected for use in a structural evaluation of the PADS concept. The structural evaluation tests were conducted to quantify the effects of the PADS concept on the compression-after-impact behavior of graphite-epoxy laminates. Laminate strength and failure strain are reported as a function of impact energy for both a brittle-matrix material system and a toughened-matrix material system.

Test Specimens

Two types of test specimens were used in this study. PADS constituent specimens were impacted to evaluate the performance of several face-sheet/core combinations. PADS concept evaluation specimens were compression loaded to determine the effects of the PADS concept on the compression-after-impact behavior of a laminate.

Constituent Specimens

The constituent specimens were fabricated using a face-sheet material, a core material, and a base laminate material. Four commercially available thermosetting materials were chosen as face-sheet candidates. These materials were Du Pont Kevlar-49/Fiberite MXM-7714 (written as Ke/MXM-7714), Ferro S-glass/293, Hercules AS4/3501-6, and Hercules AS4/American Cyanamid HST-7 (written as AS4/HST-7). These materials were selected because they represent a tough fiber, a cost-effective fiber, a brittle graphite-epoxy laminate, and a toughened graphite-epoxy laminate, respectively. The first three materials were 10-mil-thick, plain-weave preimpregnated cloth, and the AS4/HST-7 material was 5.5-mil-thick, unidirectional preimpregnated tape. Each cloth material was laid up to form 3-ply laminates approximately 0.030 in. thick. The stacking sequence for these laminates was $[+45/0/-45]_t$. The unidirectional tape was laid up to form 6-ply laminates approximately 0.033 in. thick. The stacking sequence for these laminates was $[\pm 45/0/90/\mp 45]_t$. Preliminary testing with 0.020-in-thick face sheets indicated that 0.030-in-thick face sheets were needed to achieve significant damage reduction.

Four commercially available materials were chosen as PADS core candidates. These materials were aluminum honeycomb and Du Pont Nomex honeycomb (each 8.0 lb/ft^3), Rohr 110WF Rohacell foam (6.9 lb/ft^3), and multiple layers of American Cyanamid FM-73 adhesive (total weight 8.0 lb/ft^3). The aluminum core was chosen because it offered plastic deformability. The Nomex core was chosen because of its common usage in composite structures. The Rohacell core was chosen because of its uniform small cell size and ease of machining. The layered FM-73 adhesive was chosen because of its compactness. The core was 0.25 in. thick except for selected cases with a 0.125-in-thick core and layered FM-73 adhesive. In the latter case the thickness was chosen to provide a weight approximately equal to the 0.25-in-thick core materials. Preliminary testing on lower density core materials indicated the need for core densities at least in the range from 7 to 8 lb/ft^3.

The base laminate material was AS4/3501-6 graphite-epoxy preimpregnated tape. These tapes were laid up to form 48-ply laminates approximately 0.25 in. thick, and the laminate stacking sequence was $[+45/0/-45/90]_{6s}$.

All laminates were cured in an autoclave using the manufacturers' recommended procedures. Following cure, the laminates were ultrasonically C-scanned to establish specimen quality. The face sheets and cores were cut to 4 in. squares, and the base laminates were cut to 5 in. squares. Each face-sheet/core combination was centered on a base laminate, and the face sheet, core, and base laminate were bonded using FM-73 adhesive. The PADS constituent specimens evaluated in this study are summarized in table 1. A total of 105 constituent specimens were tested.

Concept Evaluation Specimens

The concept evaluation specimens consist of base laminates with the test section protected by a PADS concept. The PADS concept was the same for all the evaluation specimens and was selected based on the constituent specimen results. The PADS concept covered a 4-in-square area. The base laminates were fabricated using either AS4/3501-6 or AS4/HST-7 graphite-epoxy materials. Preimpregnated tapes were laid up to form 48-ply laminates. The stacking sequence for all the AS4/3501-6 and for most of the AS4/HST-7 laminates was $[\pm 45/0_2/\mp 45/90_2]_{3s}$. Some of the AS4/HST-7 laminates were inadvertently fabricated as $[\pm 45/0_2/\mp 45/90_2/\pm 45/90_2/\mp 45/90_2/\pm 45/0_2/\mp 45/90_4/\pm 45/90_2/\mp 45/90_2/\pm 45/90/0/\mp 45/90_2/\pm 45/90_2/\mp 45]_t$ laminates. The stacking sequence for these unsymmetric laminates was determined using a deply technique (ref. 5). The AS4/3501-6 and AS4/HST-7 laminates were nominally 0.25 in. thick and 0.31 in. thick, respectively. All the AS4/3501-6 and most of the AS4/HST-7 laminates were 10.0 in. long and 5.0 in. wide. Some of the AS4/HST-7 laminates were 10 in. long and 7.0 in. wide. Concept evaluation specimens having AS4/3501-6 base laminates are subsequently referred to herein as 3501-6 specimens, and concept evaluation specimens having AS4/HST-7 base laminates are subsequently referred to as HST-7 specimens. A total of 74 concept evaluation specimens were tested.

Apparatus and Tests

Impacts

Specimens were impacted on the PADS-protected region using either a projectile from a compressed air gun or a dropped weight. A procedure for air-gun impacting graphite-epoxy components is detailed in reference 6, and this procedure was used in the current investigation. Aluminum spheres 0.5 in. in diameter were used as impact projectiles. These spheres were propelled by a compressed air gun equipped with an electronic detector to measure projectile speed. A schematic drawing of the air gun and a description of its operation are also given in reference 6. For convenience, this type of impact is subsequently referred to as a projectile impact. Projectile impacts were performed at speeds ranging from approximately 100 to 500 ft/sec which correspond to impact energies from 1.0 to 25.5 ft-lb, respectively. Dropped-weight impacts were performed using a 10-lb weight with a 0.5-in-diameter hemispherical head at energy levels ranging from 4.0 to 50.0 ft-lb. The projectile and dropped weight were directed normal to the plane of the specimen, and all specimens were impacted at the center of the PADS-protected region. Specimen edges were supported by fixtures during impacting. An example of such a fixture is the test fixture shown in figure 1.

Compression Loading

Concept evaluation specimens were loaded in axial compression using a 300-kip-capacity hydraulic testing machine. The loaded ends of the specimen were clamped by fixtures during testing, and the unloaded sides were simply supported by restraints to prevent the specimen from buckling as a wide column. All specimens were tested to failure by gradually applying a compressive load to simulate a static loading condition. A typical specimen mounted in the support fixture is shown in figure 1.

Electrical resistance strain gauges were used to monitor strains, and direct-current differential transformers were used to monitor longitudinal displacements of the specimen ends. Electrical signals from the instrumentation and the corresponding applied loads were recorded on magnetic tape at regular time intervals during the test.

Results and Discussion

This section describes results from the constituent tests and from the concept evaluation tests. Combinations of the PADS constituents were evaluated on the basis of damage visibility and damage protection to determine the most effective PADS configuration. This PADS concept was evaluated to determine the effects of impact damage on the compression-after-impact response of composite laminates.

Constituent Tests

Impact-site damage visibility. The ease with which a critical impact site can be located was the first criterion by which the PADS designs were evaluated. The PADS designs were qualitatively rated visually, and the indentation depths were measured.

Photographs of impacted surfaces are shown in figure 2 for a woven Kevlar-Rohacell foam PADS configuration. These photographs illustrate the impact-site visibility for five impact energy levels. Labels having energy levels accompanied by speeds are for specimens with air-gun projectile impacts. Labels having only energy levels are for specimens with dropped-weight impacts. The woven fiberglass face sheets provided visibility at the lowest impact levels because of surface crazing. The woven graphite-epoxy face sheets provided slightly inferior visibility. All core materials performed acceptably well with the exception of the layered FM-73 adhesive core which gave only marginal visibility improvement compared with a specimen without PADS. The impact sites for the specimens without PADS were not visible at any energy level.

Surface indentation depths were measured and are categorized by core material and impact energy level in figure 3. The impact sites were visually classified qualitatively and then related to the indentation depths as shown below:

Indentation depth, in.	Visibility
<0.008	Not visible
>0.008 and <0.040	Barely visible
>0.040 and <0.080	Visible
>0.080	Easily visible

The height of the bar in figure 3 represents the range of indentation depths measured for the four face-sheet materials. The layered FM-73 adhesive core material is ineffective for improving damage visibility. The other three core materials perform about equally well, with the aluminum honeycomb being slightly more effective than the other two.

The surface indentation data are also affected by the PADS face-sheet material, and these data are plotted in figure 4. The height of the bars on this figure represents the range of indentation depths measured for the three acceptable core materials. The data for the layered FM-73 adhesive specimens are not plotted. In all but one case, the woven Kevlar face sheet provided the most damage visibility when indicated by indentation depth.

Damage protection. Average damage areas were measured from C-scans of constituent specimen base laminates. Micrographs of selected specimens confirmed the C-scan results. The measured damage areas are summarized in figure 5 where they are categorized with respect to core material versus impact energy level. The height of the bars in this figure represents the range of damage measured for the four face-sheet materials. The data show that the layered FM-73 adhesive core and the thinner (0.125-in.) Rohacell and Nomex cores are ineffective in reducing damage to the base laminate. The 0.25-in-thick Rohacell, Nomex, and aluminum honeycomb cores all performed well. The Nomex and Rohacell cores were slightly more effective than the aluminum honeycomb core since both cores eliminated damage at the intermediate impact energy levels and reduced the damage area by approximately 50 percent at the highest impact energy level.

The damage-area data are also affected by the face-sheet material of a configuration, and these data are plotted in figure 6. The data for the layered FM-73 adhesive core and the thin (0.125-in.) cores are not included because of their poor performance. The height of the bars in this figure represents the range of damage for the acceptable core materials. The four face-sheet materials have an essentially equal performance with respect to damage protection. The AS4/HST-7 tape and the Kevlar cloth face-sheet materials appear to be slightly more effective for minimizing the damage area when compared with the other face-sheet materials.

In summary, significant damage protection was achieved with any of the face sheets combined with the Nomex or Rohacell cores. The aluminum honeycomb core was only slightly less effective.

PADS design for compression-after-impact testing. Since many of the PADS designs proved to be effective in both increasing impact-site visibility and providing damage protection to the structural laminate, the selection of a design for further evaluation was based somewhat on secondary considerations. Kevlar cloth was selected as the face-sheet material because of its excellent performance in both primary evaluations and because of its low weight and ease of fabrication. Rohacell foam (0.25 in. thick, 110WF) was selected as the core material because of its excellent performance, its ease of fabrication, and its slight weight advantage as compared with the honeycomb cores.

Concept Evaluation

Failure data for the concept evaluation specimens indicate a significant effect of the PADS concept on

the compression-after-impact (CAI) behavior of a laminate. Results are presented in tables 2–8 and figures 7–10 for specimen strength and failure strain. The failure data do not appear to be a function of the method used to impact the specimen. Also, the unsymmetric stacking sequence for some laminates does not appear to affect the failure results. The strength and failure strain data are plotted as a function of impact energy for the 3501-6 specimens in figures 7 and 8 and for the HST-7 specimens in figures 9 and 10. The symbols in the figures correspond to the experimental data, and the solid lines are lower bounds for these data. The results in the figures show that as the impact energy increases, the laminates without the PADS concept have CAI failure strains that approach 0.40 percent for the 3501-6 specimens in this study and 0.50 percent for the HST-7 specimens in this study. For the impact emergies considered, the laminates with the PADS concept have CAI failure strains greater than 0.60 percent for the 3501-6 specimens in this study and greater than 0.85 percent for the HST-7 specimens in this study. These failure strain data demonstrate a 50-percent improvement in CAI failure strain for the 3501-6 specimens and a 70-percent improvement in the CAI failure strain for the HST-7 specimens. These improvements are a direct result of the PADS concept.

The structural efficiency of the selected PADS concept for AS4/HST-7 laminates is shown in figure 11. Results are presented for a weight index W/AL (where W is the structural weight, A is the cross-sectional area, and L is the laminate length) versus a load index N_x/L (where N_x is the compressive stress resultant). These results were obtained using the PASCO panel analysis and sizing computer program (ref. 7). The 0.003 in/in. strain has been used as a maximum design strain for brittle-matrix composite structures. The 0.006 in/in. strain is a typical design strain for heavily loaded wing structures. A simple conservative calculation to approximate the weight of a composite structure with the PADS concept indicates that the weight of the PADS concept is approximately 17 percent of the structural weight. This calculation is based on considering a flat, 48-ply (0.31-in-thick) laminate. The laminate has an areal weight of 2.68 lb/ft^2, and the PADS concept has an areal weight of 0.46 lb/ft^2. The analytical structural efficiency results shown in the figure reflect the 17-percent increase in structural weight for structures with the PADS concept and with a 0.006 in/in. max-

imum design strain. The results in the figure show that the heavily loaded structures with the PADS concept are more structurally efficient than the heavily loaded structures with a 0.003 in./in. maximum design strain and without the PADS concept. The weight of the PADS concept for structures loaded by $N_x/L > 250$ lb/in^2 is more than offset by the structural weight savings from using a 0.006 in/in. maximum design strain. The PADS concept appears to be an effective damage-tolerant concept that will allow higher ultimate strain designs for heavily loaded composite structures without significant weight increases.

Concluding Remarks

A protection and detection surface (PADS) concept has been studied for application to composite primary aircraft structures. The PADS concept utilizes a lightweight sandwich construction, and combinations of four face sheets and four cores were evaluated on the basis of damage visibility and damage protection. The $[+45/0/-45]_t$ Kevlar-epoxy woven face sheet with a 110WF Rohacell foam core was found to be the most effective PADS configuration among those configurations evaluated. This PADS configuration was bonded to AS4/3501-6 and AS4/HST-7 base laminates to assess the effect of the PADS concept on the compression-after-impact (CAI) behavior of a laminate. For the impact conditions studied, the failure strain data demonstrate a 50-percent improvement in CAI failure strain for the 3501-6 specimens and a 70-percent improvement in the CAI failure strain for the HST-7 specimens. These improvements are a direct result of the PADS concept. A simple conservative calculation to approximate the weight of a composite structure with the PADS concept indicates that the weight of the PADS concept is approximately 17 percent of the structural weight. The weight of the PADS concept for heavily loaded composite structures is more than offset by the structural weight savings that result from increased maximum design strains. The PADS concept appears to be an effective damage-tolerant concept that will allow higher ultimate strain designs for heavily loaded composite structures without significant weight increases.

References

1. Williams, Jerry G.; O'Brien, T. Kevin; and Chapman, A. J., III: Comparison of Toughened Composite Laminates Using NASA Standard Damage Tolerance Tests. *ACEE Composite Structures Technology—Review of Selected NASA Research on Composite Materials and Structures*, NASA CP-2321, 1984, pp. 51–73.

2. Dexter, H. Benson; and Funk, Joan G.: Impact Resistance and Interlaminar Fracture Toughness of Through-the-Thickness Reinforced Graphite/Epoxy. *A Collection of Technical Papers—AIAA/ASME/ASCE/AHS 27th Structures, Structural Dynamics and Materials Conference, Part 1,* 1986, pp. 700–709. (Available as AIAA-86-1020.)

3. Johnston, Norman J.; and Hergenrother, Paul M.: *High Performance Thermoplastics: A Review of Neat Resin and Composite Properties.* NASA TM-89104, 1987.

4. Haftka, Raphael T.; Starnes, James, H., Jr.; and Nair, Sudhakar: Design for Global Damage Tolerance and Associated Mass Penalties. *J. Aircr.,* vol. 20, no. 1, Jan. 1983, pp. 83–88.

5. Freeman, S. M.: Characterization of Lamina and Interlaminar Damage in Graphite/Epoxy Composites by the Deply Technique. *Composite Materials: Testing and Design (Sixth Conference),* I. M. Daniel, ed., ASTM Spec. Tech. Publ. 787, c.1982, pp. 50–62.

6. Starnes, J. H., Jr.; Rhodes, M. D.; and Williams, J. G.: Effect of Impact Damage and Holes on the Compressive Strength of a Graphite/Epoxy Laminate. *Nondestructive Evaluation and Flaw Criticality for Composite Materials.* R. B. Pipes, ed., ASTM Spec. Tech. Publ. 696, c.1979, pp. 145–171.

7. Anderson, Melvin S.; and Stroud, W. Jefferson: A General Panel Sizing Computer Code and Its Application to Composite Structural Panels. *AIAA J.,* vol. 17, no. 8, Aug. 1979, pp. 892–897.

Table 1. PADS Configurations for Constituent Tests

Specimen	Face-sheet material (a)	Face-sheet lay-up	Core thickness, in.	Core material (b)
C1	Kevlar	$[\pm 45/0/-45]_t$	0.25	A
C2			.25	N
C3			.25	R
C4			.035	AD
C5	Glass		.25	A
C6			.25	N
C7			.25	R
C8			.035	AD
C9	Graphite		.25	A
C10			.25	N
C11			.25	R
C12			.035	AD
C13	Tape	$[\pm 45/0/90/\mp 45]_t$	.25	A
C14			.25	N
C15			.25	R
C16			.035	AD
C17	Tape		.125	N
C18	Tape		.125	R
C19	Kevlar	$[+45/0/-45]_t$	.125	N
C20	Kevlar	$[+45/0/-45]_t$	.125	R

[a]Kevlar: Ke/MXM-7714; 10-mil-thick plain-weave cloth.
Glass: S-glass/293; 10-mil-thick plain-weave cloth.
Graphite: AS4/3501-6; 10-mil-thick plain-weave cloth.
Tape: AS4/HST-7; 5.5-mil-thick tape.

[b]A: aluminum honeycomb, 8.0 lb/ft^3.
N: Nomex honeycomb, 8.0 lb/ft^3.
R: 110WF Rohacell, 6.9 lb/ft^3.
AD: multiple layers of FM-73 adhesive, 8.0 lb/ft^3.

Table 2. Failure Data for AS4/3501-6 Specimens Without PADS
Impacted Using a Dropped Weight

Specimen	Impact energy, ft-lb	Strength, ksi
DW1-1	20.0	25.7
DW1-2	20.0	25.5
DW1-3	20.0	26.5
DW1-4	31.3	20.1
DW1-5	31.3	23.7
DW1-6	31.3	21.2
DW1-7	50.0	18.5
DW1-8	50.0	18.9
DW1-9	50.0	19.5

Table 3. Failure Data for AS4/3501-6 Specimens Without PADS Impacted Using
a Projectile From a Compressed Air Gun

Specimen	Impact energy, ft-lb	Strength, ksi	Failure strain, percent (a)
G1-1	4.1	56.6	(b)
G1-2	4.2	58.8	(b)
G1-3	4.0	48.4	(b)
G1-4	8.9	30.5	(b)
G1-5	9.3	26.8	(b)
G1-6	9.2	30.9	(b)
G1-7	17.2	25.5	0.45
G1-8	16.5	25.3	.47
G1-9	16.3	26.0	.46
G1-10	25.3	19.8	.41
G1-11	24.8	19.7	.41
G1-12	-25.1	21.2	.41

[a]Failure strain was calculated using laminate end-shortening and original length rather than being measured by strain gauges.
[b]Failure strain data unavailable.

Table 4. Failure Data for AS4/3501-6 Specimens With PADS Impacted Using
a Projectile From a Compressed Air Gun

Specimen	Impact energy, ft-lb	Strength, ksi	Failure strain, percent (a)
G1-13	16.1	63.4	1.08
G1-14	16.5	60.7	1.06
G1-15	16.7	64.9	1.09
G1-16	24.4	39.2	.69
G1-17	25.2	40.4	.68
G1-18	24.8	32.1	.64

[a]Failure strain was calculated using laminate end-shortening and original length rather than being measured by strain gauges.

Table 5. Failure Data for AS4/HST-7 Specimens Without PADS Impacted
Using a Dropped Weight

Specimen	Impact energy, ft-lb	Strength, ksi	Failure strain, percent (a)
DW2-1	0	58.2	1.24
DW2-2	14.1	63.6	(b)
DW2-3	14.1	57.4	1.22
DW2-4	14.1	53.9	1.07
DW2-5	16.9	59.3	1.38
DW2-6	22.6	41.9	(b)
DW2-7	22.6	41.5	(b)
DW2-8	24.0	49.9	1.07
DW2-9	31.3	33.2	.69
DW2-10	31.3	35.1	.71
DW2-11	31.3	34.1	.70
DW2-12	50.0	25.8	.53
DW2-13	50.0	25.5	.51
DW2-14	50.0	27.2	.54
DW2-15	c50.0	26.1	.56
DW2-16	c50.0	26.7	.57
DW2-17	c50.0	28.2	.55

aFailure strain was calculated using laminate end-shortening and original length rather than being measured by strain gauges.
bFailure strain data unavailable.
cImpact event: 9.0 ft-lb followed by 50.0 ft-lb.

Table 6. Failure Data for AS4/HST-7 Specimens With Pads Impacted
Using a Dropped Weight

Specimen	Impact energy, ft-lb	Strength, ksi	Failure strain, percent (a)
DW2-18b	22.6	54.2	1.28
DW2-19b	22.6	51.0	1.19
DW2-20b	22.6	50.7	1.20
DW2-21b	31.3	56.4	1.34
DW2-22b	31.3	57.2	1.36
DW2-23b	31.3	40.9	.92
DW2-24	50.0	42.7	.87
DW2-25	50.0	49.8	1.02
DW2-26	50.0	44.6	.92

aFailure strain was calculated using laminate end-shortening and original length rather than being measured by strain gauges.
bBase laminate unsymmetric.

Table 7. Failure Data for AS4/HST-7 Specimens Without PADS Impacted Using
a Projectile From a Compressed Air Gun

Specimen	Impact energy, ft-lb	Strength, ksi	Failure strain, percent (a)
G2-1	0	71.0	(b)
G2-2	5.6	62.9	(b)
G2-3	5.7	64.9	(b)
G2-4	9.2	59.0	(b)
G2-5	9.3	48.2	(b)
G2-6	9.2	59.6	(b)
G2-7	9.2	57.7	(b)
G2-8	9.4	59.6	1.24
G2-9	9.5	61.1	1.31
G2-10[c]	15.8	47.2	.97
G2-11[c]	15.6	42.7	.85
G2-12[c]	16.0	41.2	.75
G2-13[c]	25.4	37.1	.68
G2-14[c]	25.0	37.3	.70
G2-15[c]	25.0	39.0	.74

[a]Failure strain was calculated using laminate end-shortening and original length rather than
being measured by strain gauges.
[b]Failure strain data unavailable.
[c]Specimen dimensions: 7 in. long by 10 in. wide; specimens buckled prior to failure.

Table 8. Failure Data for AS4/HST-7 Specimens With PADS Impacted Using
a Projectile From a Compressed Air Gun

Specimen (a)	Impact energy, ft-lb	Strength, ksi	Failure strain, percent (b)
G2-16	16.0	54.4	1.28
G2-17	16.2	53.2	1.25
G2-18	17.4	52.0	1.22
G2-19	24.8	55.8	1.33
G2-20	25.0	53.6	1.26
G2-21	24.3	56.4	1.34

[a]Base laminate unsymmetric.
[b]Failure strain was calculated using laminate end-shortening and original length rather than
being measured by strain gauges.

9

Protection and detection surface (PADS)
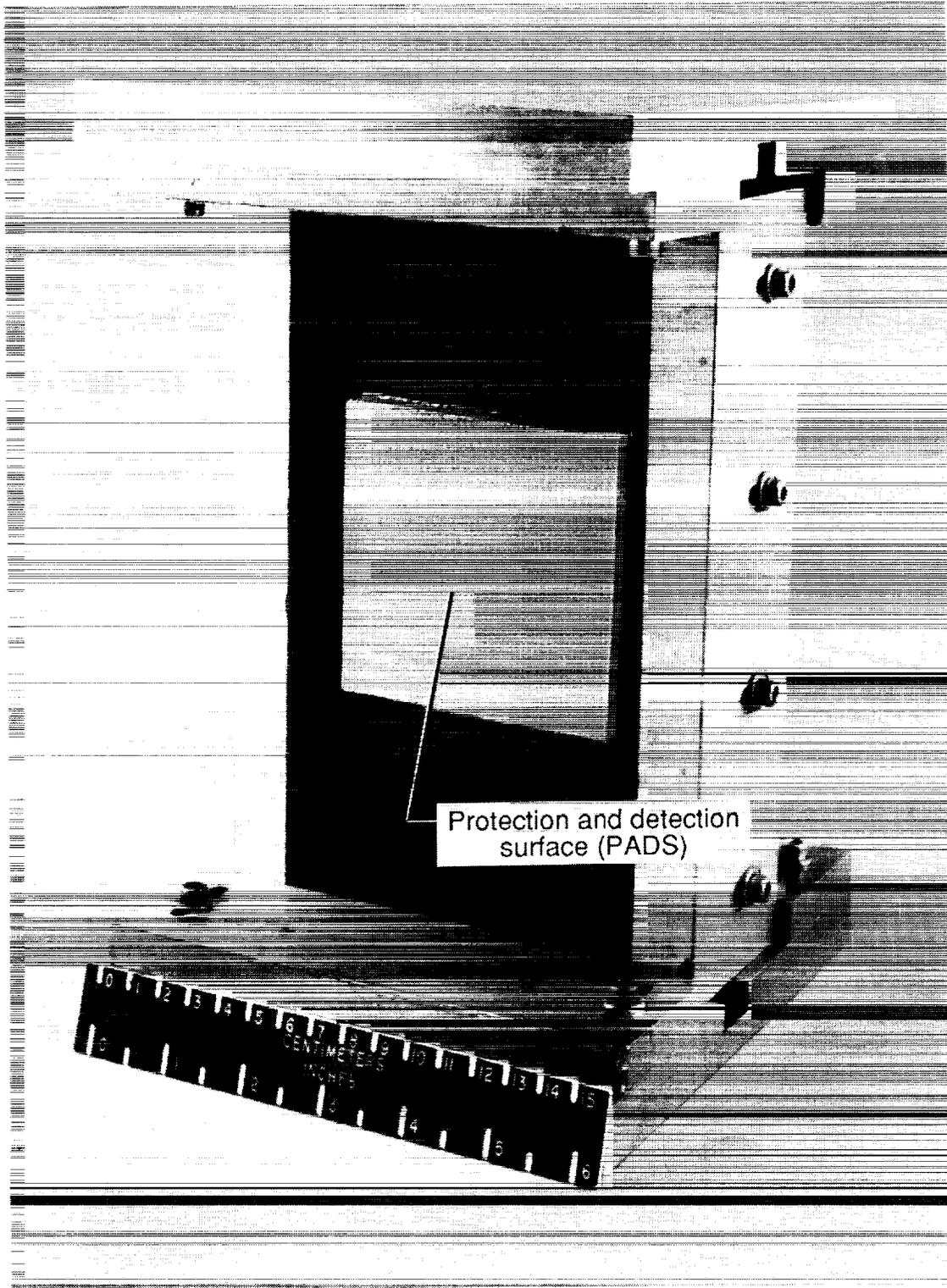
L-89-12797

Figure 1. Evaluation specimen of PADS concept in test fixture.
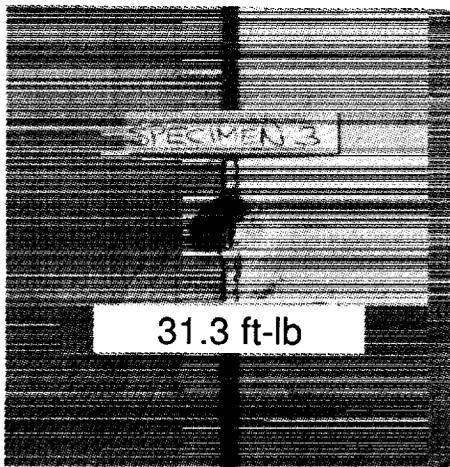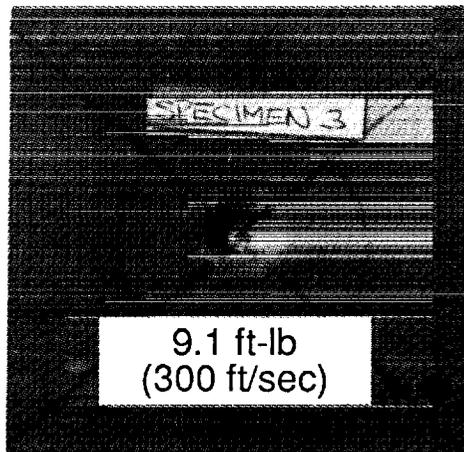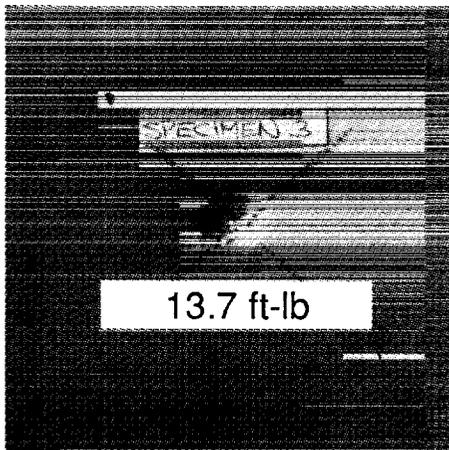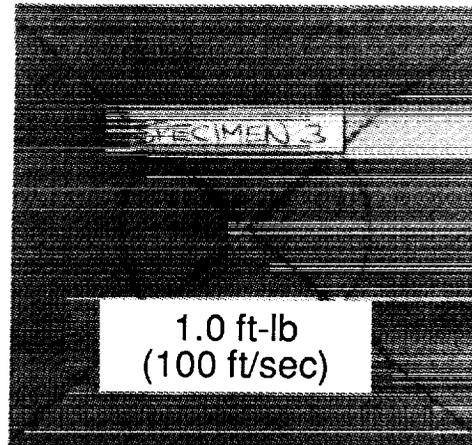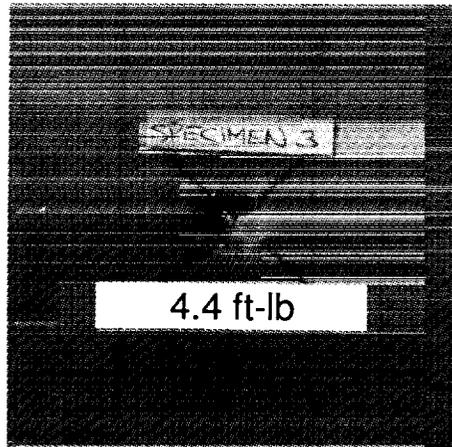
L-90-27

Figure 2. Impact site visibility for woven Kevlar-Rohacell foam PADS configuration.
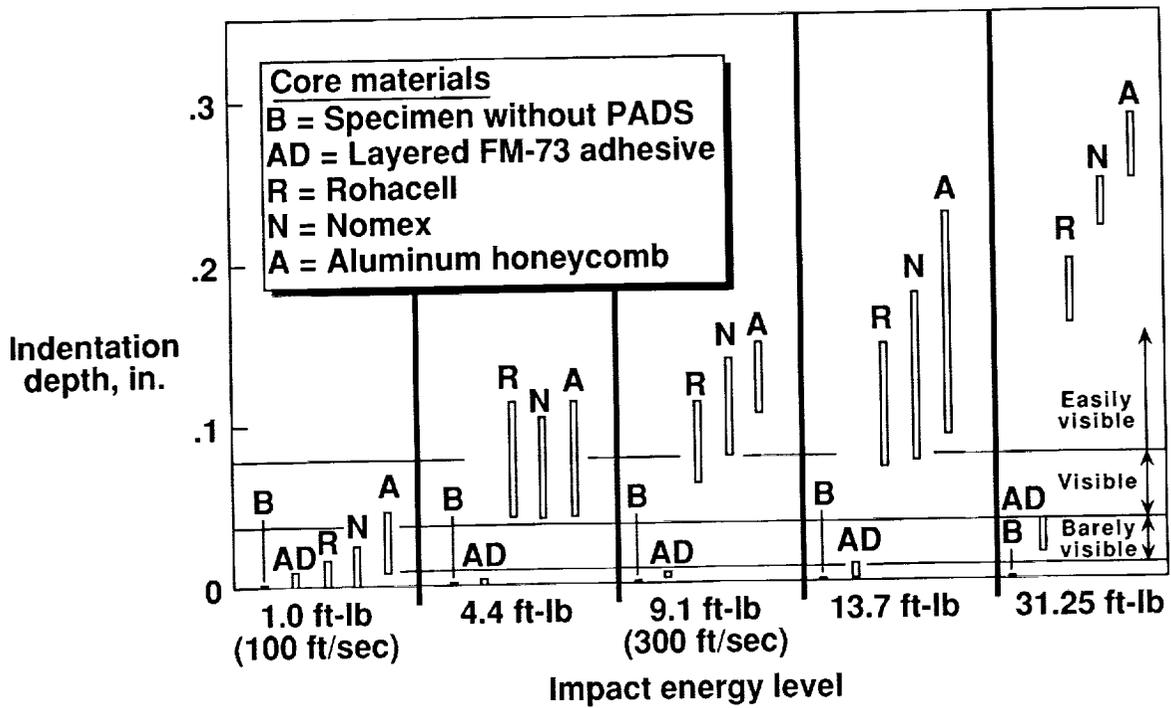
Figure 3. Surface indentation depths for core materials.
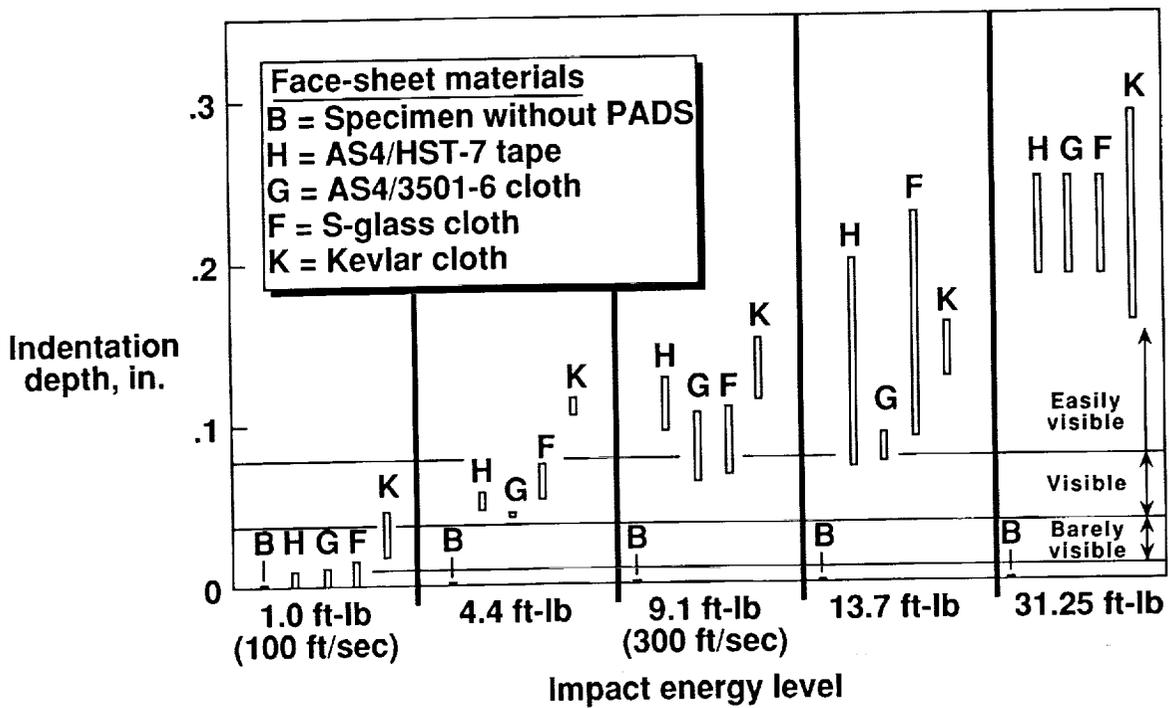
Figure 4. Surface indentation depths for face-sheet materials.
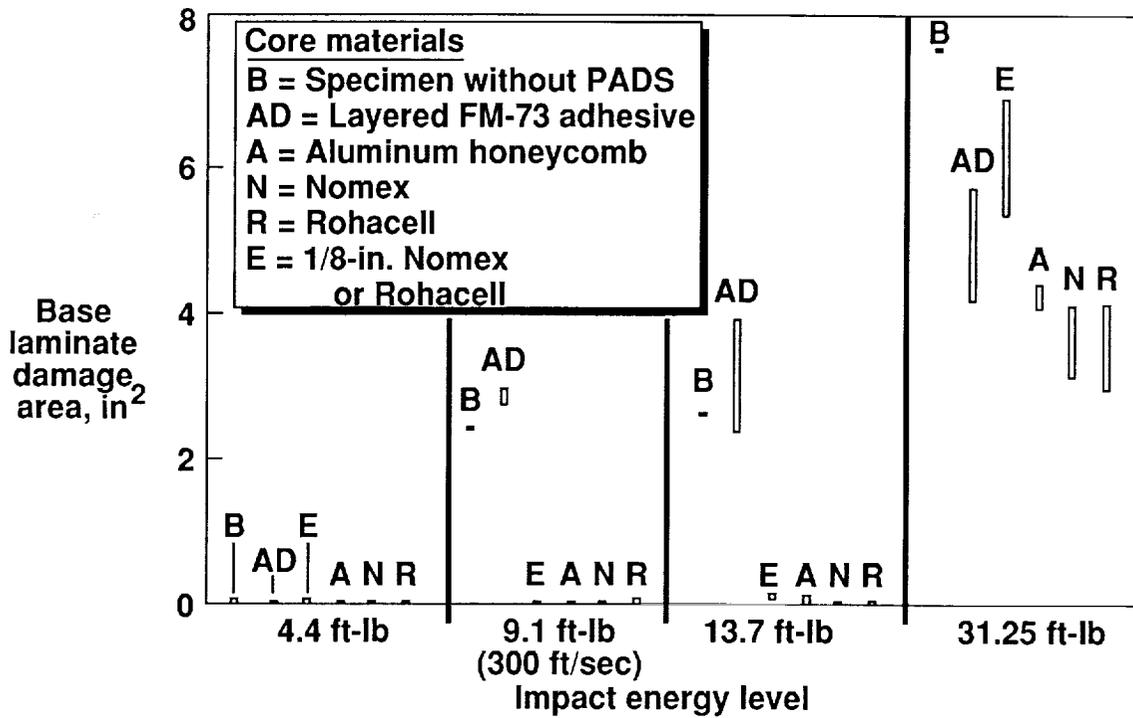
Figure 5. Effect of core materials on damage area for base laminate.
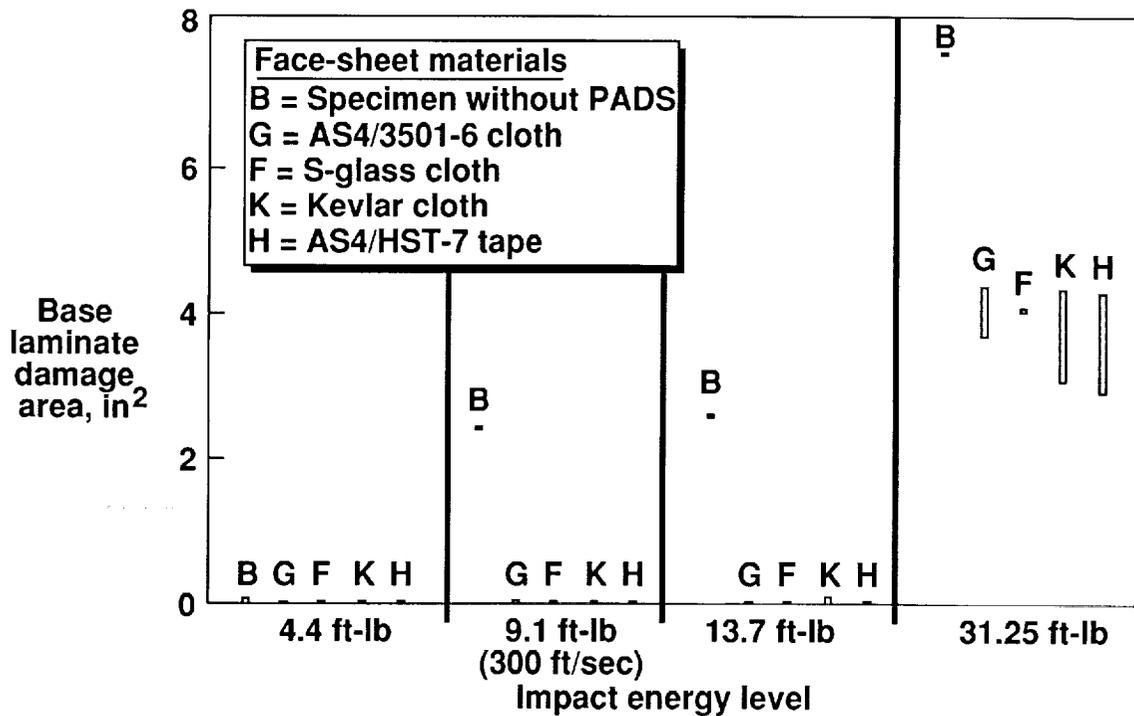
Figure 6. Effect of face-sheet materials on damage area for base laminate.
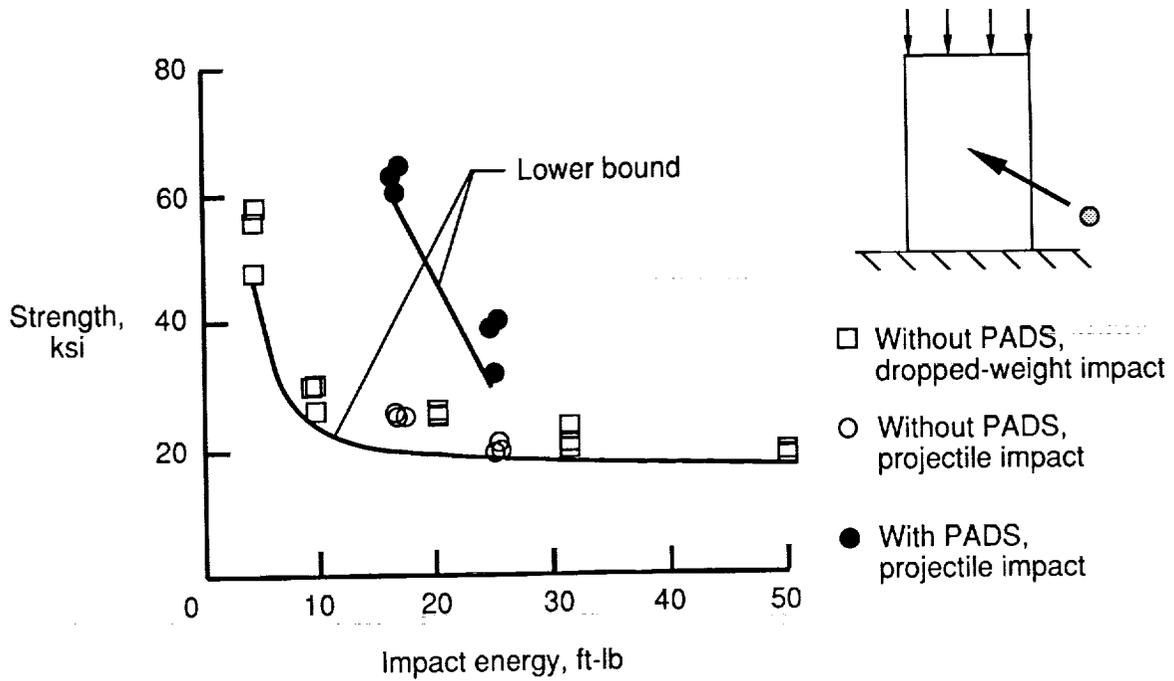
Figure 7. Strength results for impacted AS4/3501-6 specimens.
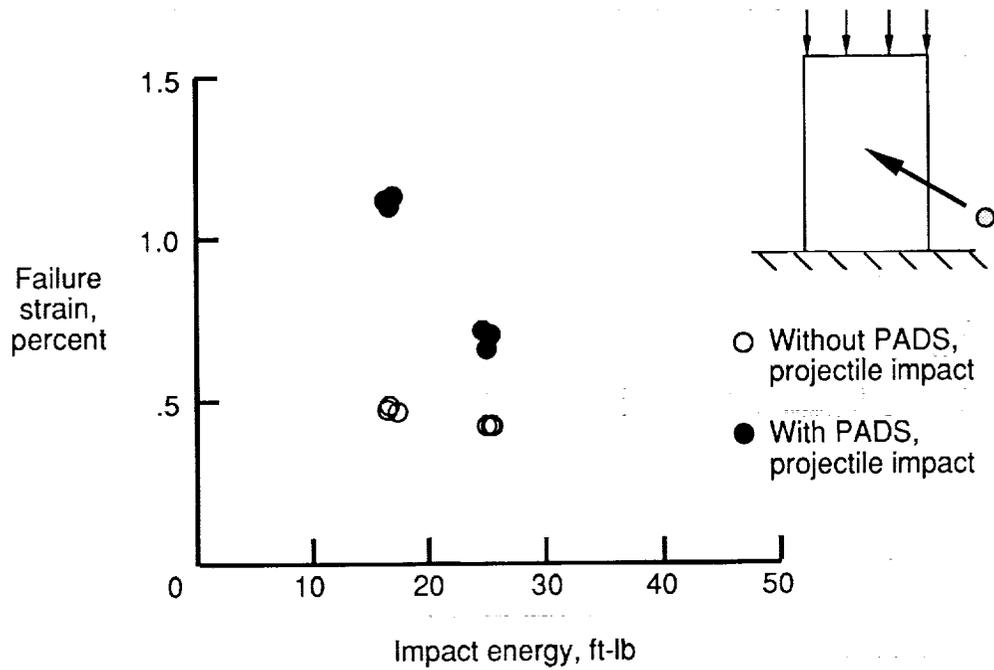
Figure 8. Results of failure strain for impacted AS4/3501-6 specimens.
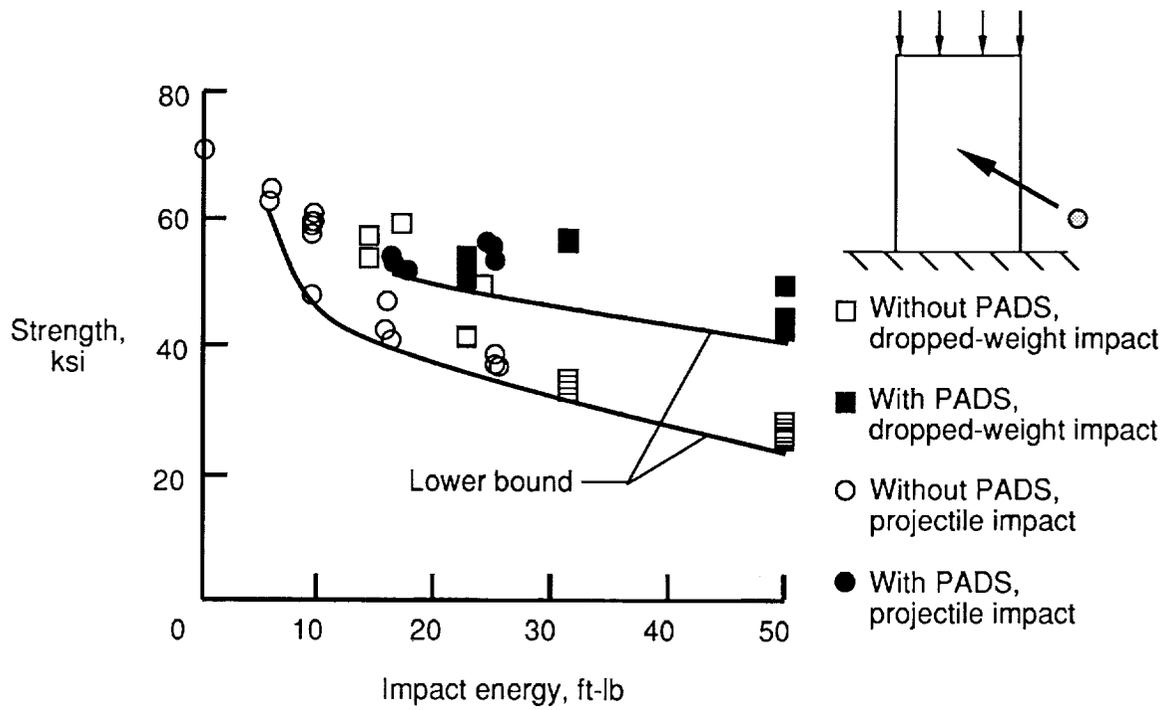
Figure 9. Strength results for impacted AS4/HST-7 specimens.
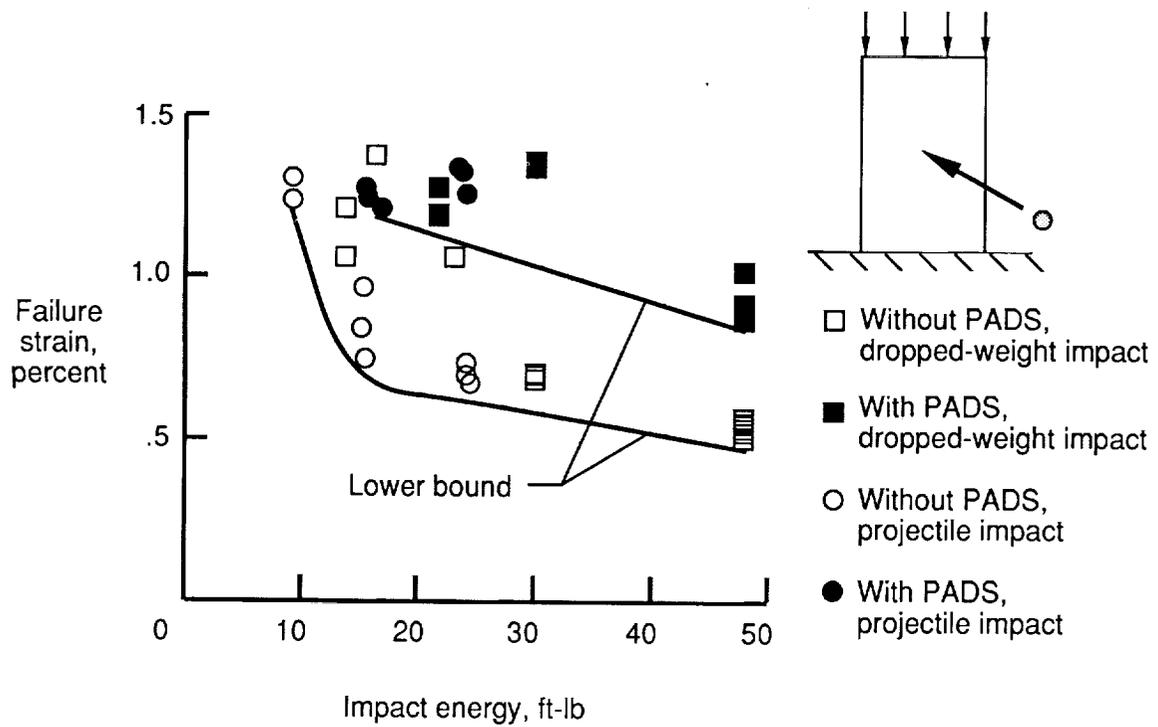
Figure 10. Results of failure strain for impacted AS4/HST-7 specimens.
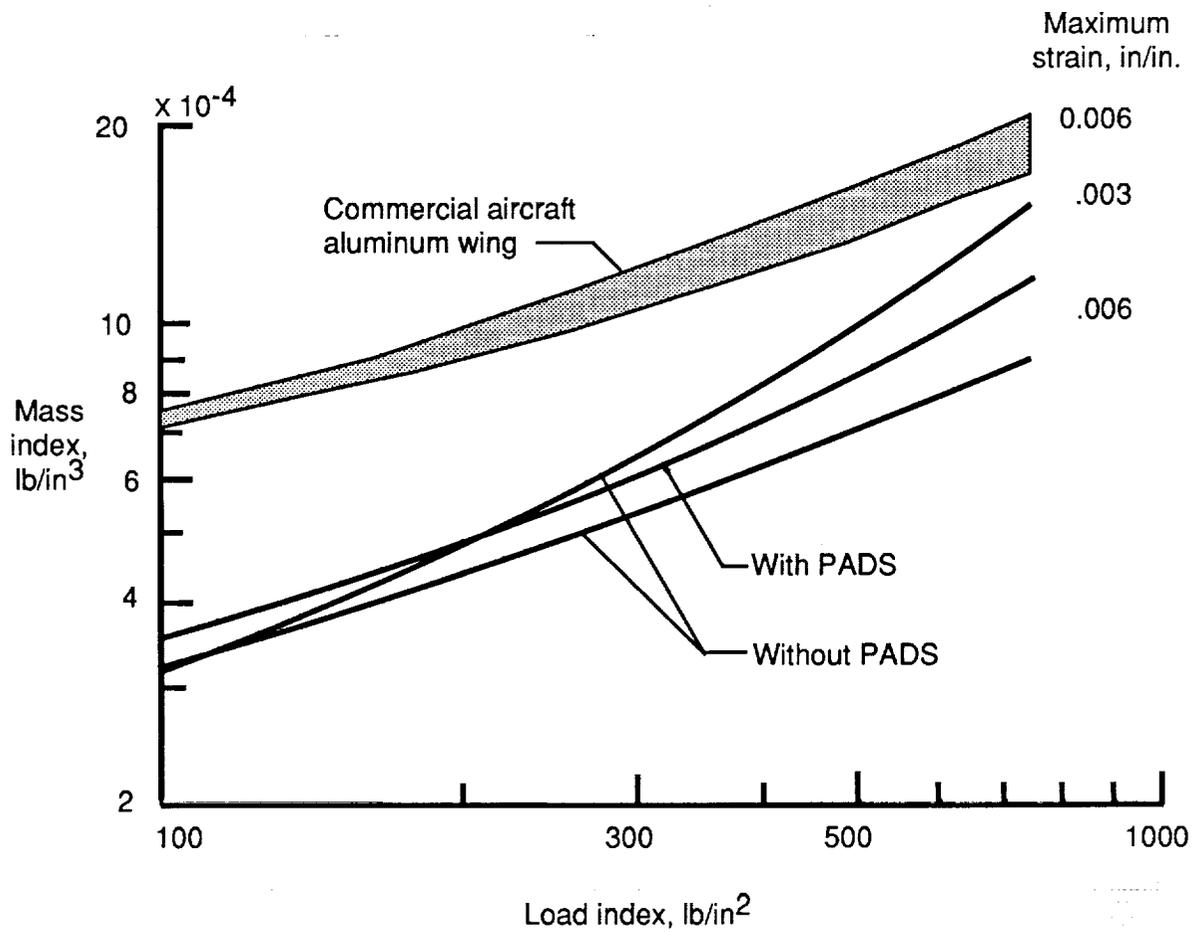
Figure 11. Effect of PADS concept on structural efficiency.

Report Documentation Page

1. Report No. NASA TP-3011	2. Government Accession No.	3. Recipient's Catalog No.

4. Title and Subtitle	5. Report Date
A Protection and Detection Surface (PADS) for Damage Tolerance	September 1990
	6. Performing Organization Code

7. Author(s)	8. Performing Organization Report No.
Mark J. Shuart, Chunchu B. Prasad, and Sherrill B. Biggers	L-16775

9. Performing Organization Name and Address	10. Work Unit No.
NASA Langley Research Center Hampton, VA 23665-5225	510-02-21-01
	11. Contract or Grant No.

12. Sponsoring Agency Name and Address	13. Type of Report and Period Covered
National Aeronautics and Space Administration Washington, DC 20546-0001	Technical Paper
	14. Sponsoring Agency Code

15. Supplementary Notes

16. Abstract

A concept for a protection and detection surface (PADS) has been studied for application to composite primary aircraft structures. A Kevlar-epoxy woven face sheet with a Rohacell foam core was found to be the most effective PADS configuration among the configurations evaluated. The weight of the PADS configuration was estimated to be approximately 17 percent of the structural weight. The PADS configuration was bonded to graphite-epoxy base laminates, and up to a 70-percent improvement was observed in compression-after-impact failure strains.

17. Key Words (Suggested by Authors(s))	18. Distribution Statement
Composite materials Damage tolerance Sandwich construction Compression Impact	Unclassified—Unlimited Subject Category 24

19. Security Classif. (of this report)	20. Security Classif. (of this page)	21. No. of Pages	22. Price
Unclassified	Unclassified	17	A03